Science of the Total Environment 644 (2018) 430–438

Contents lists available at ScienceDirect

Science of the Total Environment

journal homepage: www.elsevier.com/locate/scitotenv

Crystal violet and toxicity removal by adsorption and simultaneous photocatalysis in a continuous flow micro-reactor

Olga Sacco [a], Mariantonietta Matarangolo [a], Vincenzo Vaiano [a,*], Giovanni Libralato [b], Marco Guida [b], Giusy Lofrano [c], Maurizio Carotenuto [c]

[a] Department of Industrial Engineering, University of Salerno, via Giovanni Paolo II, 132, 84084 Fisciano, SA, Italy
[b] Department of Biology, University of Naples Federico II, via Cinthia ed. 7, 80126 Naples, Italy
[c] Department of Chemical and Biology, University of Salerno, via Giovanni Paolo II 132, 84084 Fisciano, SA, Italy

HIGHLIGHTS

- A continuous flow micro-reactor irradiated by UV-LEDs was developed.
- Removal of crystal violet dye through simultaneous adsorption and photocatalysis.
- ZnO/zeolite pellets were used as active material.
- Treated water showed a significant reduction of toxicity.
- A preliminary mathematical model was developed.

GRAPHICAL ABSTRACT

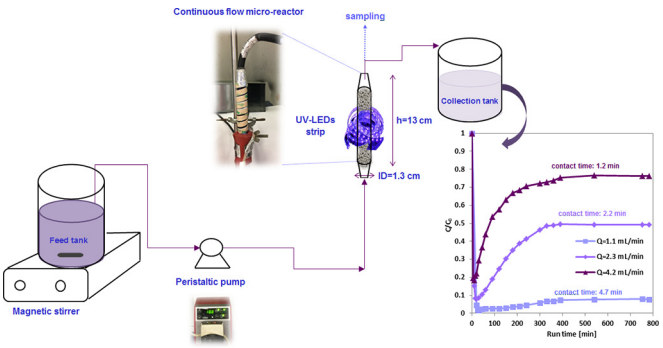

ARTICLE INFO

Article history:
Received 25 May 2018
Received in revised form 29 June 2018
Accepted 29 June 2018
Available online 6 July 2018

Editor: Zhen (Jason) He

Keywords:
Photocatalysis/adsorption
Photocatalytic micro-reactor
Zeolite
ZnO
Crystal violet
Toxicity

ABSTRACT

A continuous flow micro-reactor irradiated by UV-LEDs was employed to treat coloured wastewater by adsorption and simultaneous photocatalysis. Zinc oxide (ZnO) immobilized on commercial zeolites pellets in spherical shape (ZEO) was used as catalytic material in a micro-reactor maximizing the photocatalyst exposition to light sources, irradiating uniformly the entire solution volume and improving the mass transfer phenomena. Experimental tests were carried out on crystal violet dye (CV) as one of the main dying agent present in textile wastewater. The comparison between adsorption and adsorption/photocatalytic tests showed that UV irradiation can achieve a steady state CV concentration value corresponding to an equilibrium condition between adsorption and photocatalytic oxidation. The higher removal efficiency (*i.e.* 93%) was observed with a liquid flow rate of 1.1 mL/min (contact time = 4.7 min; CV = 10 mg/L) under UV light irradiation. In the steady state, CV removal remained constant for the overall testing time. Bioassays evidenced that toxicity was not completely removed (*i.e.* final effluent ranked as "slight acute toxic") from wastewater suggesting its suitability for sewage collection discharge. A Dubinin Radushkevich (D-R) isotherm model was applied for studying the adsorption behaviour of ZnO/ZEO sample. CV adsorption constants were evaluated from experimental data carried out in dark conditions in a batch system. Kinetic expression of CV removal and the D-R adsorption were incorporated in the CV mass balance estimating the kinetic parameter. The model was validated comparing the calculated CV conversion with the experimental tests collected at different CV inlet concentration.

* Corresponding author.
E-mail address: vvaiano@unisa.it (V. Vaiano).

https://doi.org/10.1016/j.scitotenv.2018.06.388
0048-9697/

1. Introduction

Several industries such as textiles, paint, ink, plastics, paper and cosmetics use different types of organic dyes and about 15% of them are lost during synthesis and processing with wastewater (Nagaveni et al., 2004; Robinson et al., 2001; Vacchi et al., 2017). The discharge of coloured wastewater in the environment is considered to be a major issue because conventional treatments such as biological methods, flocculation, coagulation, precipitation, adsorption, membrane filtration are not able to completely remove organic dyes in water (Ghaffar et al., 2018; Janoš, 2003; Pal et al., 2016; Sahoo et al., 2005). For this reason, advanced oxidation processes (AOPs) have received considerable attention in recent years to treat efficiently coloured wastewater (Li et al., 2018; Vaiano and Iervolino, 2018; Vaiano et al., 2017a). Among AOPs, heterogeneous photocatalytic methods are the most effective and attractive ones (Doong et al., 2010; Miranda et al., 2016). Photocatalysis is actually a very active area of scientific research, but its large scale implementation has not been successful so far. The main reason is attributed to the slow development of practical photocatalytic systems this means efficiently and economically viable for large-scale wastewater treatment application (Damodar and Swaminathan, 2008; Dionysiou et al., 2000). Other reasons are the absence of a proper reactor design and optimization because of the most studied photoreactors are in batch configuration (Chong et al., 2017; Liu et al., 2014a; Nguyen and Juang, 2015; Veisi et al., 2016). Reactors that could be operated in continuous mode could be a valid alternative because the main advantage is the easy scale-up of the system compared to batch processes and, therefore, they are being recently investigated by scientific literature (Damodar et al., 2010; Erdei et al., 2008; McCullagh et al., 2010). The scale-up of these types of reactors can be achieved by continuous introduction of wastewater into the reactor and by placing several devices in parallel (Cambié et al., 2016; Su et al., 2014). Among the continuous photoreactors, the use of flow micro-reactors received attention especially for photochemical applications (Schuster and Wipf, 2014). Specifically, the use of a photocatalytic micro-reactor allows to irradiate uniformly the entire solution volume and consequently, photocatalytic reactions can be substantially accelerated (from hours/days for batch process to seconds/mins in continuous-flow) (Cambié et al., 2016). Another advantage of micro-reactors is the improved mass transfer phenomena (Ray, 1999; Sengupta et al., 2001) due to the formation of a thin film of pollutant solution over the catalyst surface enabling an efficient penetration of UV radiation inside the core of the reactor too (Ollis and Turchi, 1990). In order to guarantee the continuous operation of the system, it is necessary to use semiconductors immobilized on macroscopic supports (Borges et al., 2015; Chanathaworn et al., 2014). Though the efficiency of the immobilized system may be less than that of the slurry system, the catalyst can be used continuously for a long time (Chen et al., 2001). Regarding to the immobilized systems, a variety of support materials (such as glass (Chanathaworn et al., 2014), ceramic (Vaiano et al., 2015b; Zhang et al., 2017) or polymeric substrate (Sacco et al., 2018a; Sacco et al., 2018c; Vaiano et al., 2017b)) has been studied in the last years (Kamble et al., 2004; Pozzo et al., 1997). Besides, a good choice could be the immobilization of photocatalyst on adsorbent materials to obtain hybrid catalysts (semiconductor deposited on zeolites) combining the adsorption properties of zeolite with the photocatalytic properties of the semiconductor. Several investigations have been carried out using TiO_2 or ZnO coupled with zeolites, evidencing an improvement of the photocatalytic performances compared to bulk photocatalysts (Fukahori et al., 2003; Liu et al., 2014b; Sarno et al., 2015; Susarrey-Arce et al., 2010). Most papers deal with the use of photocatalysts supported on zeolites in the powder form, thus making the development of photoreactors operating in continuous mode difficult.

Recently (Sacco et al., 2018b), the use of the simultaneous adsorption and photocatalytic processes (adsorption/photocatalysis) for the removal of caffeine was studied using zinc oxide (ZnO) photocatalyst immobilized on commercial zeolite (ZEO) as pellets (ZnO/ZEO), thus providing a suitable structured photocatalyst formulation to be used in a continuous-flow photocatalytic reactor. At our knowledge, scientific literature about the employment of a continuous-flow reactor for water depollution through the dual effect of adsorption and photocatalysis is still limited (Li et al., 2010).

This work investigated a continuous-flow micro-photoreactor using ZnO/ZEO as catalytic material. Crystal violet (CV) was selected for technology validation and assessment as one of the main widespread dying agents and its related toxicity (Adak et al., 2005; Sahoo et al., 2005; Yu et al., 2012).

2. Materials and methods

2.1. Preparation and characterization of ZnO/ZEO samples

ZnO nanoparticles (NP) has been immobilized in commercial Na-ZSM5 zeolite spherical pellets (ZEOcat Z-400, pellets size: 1.2–2 mm, SiO_2/Al_2O_3 ratio: 400, provided by ZEOCHEM) by wet impregnation method starting from $Zn(NO_3)_2 \cdot 6H_2O$ (Sigma-Aldrich) dissolved in aqueous solutions. The experimental procedure is described in our previous published work (Sacco et al., 2018b). The final ZnO loading in ZnO/ZEO composites was found to be 6.1 wt%. From the chemical-physical characterization results it was found that ZnO NPs are in wurtzite phase and incorporated in the mesoporous structure of ZEO pellets (Sacco et al., 2018b).

2.2. Photocatalytic tests using a batch reactor

The photocatalytic removal of CV was preliminarily studied in a cylindrical batch photoreactor using ZnO powder obtained from $Zn(NO_3)_2$ by thermal treatment in air at 450 °C for 2 h. A photocatalytic test, using 3 g/L of ZnO, was carried out in a Pyrex cylindrical reactor (ID = 2.6 cm, L_{TOT} = 41 cm and V_{TOT} = 200 mL). During the test an air flow rate of 144 $Ncc \cdot min^{-1}$ was continuously bubbled inside the suspension. A UV-LEDs strip (*LEDlightinghut*, nominal power: 12 W/m; main emission: 365 nm) was used as light source and positioned around the external surface of the photoreactor. The initial CV concentration was 10 mg/L while the solution volume, at the spontaneous pH (about 5.5), was 100 mL. Liquid samples were collected at fixed times and analyzed to measure the CV concentration through UV–Vis spectrophotometer (Thermo Evolution 201) at the wavelength of 583 nm (Ameen et al., 2013).

In addition to the measurement of CV concentration, mineralization of CV was evaluated in terms of total organic carbon (TOC) concentration decrease through the measurement of CO_2 obtained by catalytic combustion at T = 680 °C. CO_2 produced in gas-phase was monitored by continuous analyser (Uras 14, ABB) (Sannino et al., 2013).

2.3. Experimental tests using the continuous flow micro-reactor

The micro-reactor, which operates in continuous mode, is a cylindrical pyrex reactor (ID = 1.3 cm, L_{TOT} = 10 cm and V_{TOT} = 7 mL) because this type of geometry is the simplest configuration for a photoreactor, allowing a possible scale-up of photocatalytic systems for water and wastewater treatment.

The stock solutions containing the CV dye (at 5, 10, 15 and 25 mg/L initial concentration) were prepared and collected in the feed tank (3 L). The feed tank is equipped with a magnetic stirrer to assure the complete homogenization of the stock solution. The feed solution was pumped from the feed tank to the micro-reactor using a peristaltic pump (*Watson Marlowe 120 s*). The used liquid flow rates were 1.1, 2.3 and 4.2 mL/min. The overall liquid stream is fed from the bottom of the reactor and liquid stream passes through the catalytic bed and finally comes out from the top of the reactor, being conveyed in a tank where the treated solutions were collected. The liquid sample was withdrawn

at the outlet of the continuous flow micro-reactor. The amount of ZnO/ZEO sample, used in the experimental tests, was equal to 4 g. Starting from the bulk density (0.78 g/cm^3) and the amount of ZnO/ZEO (4 g), the volume of the catalytic bed was obtained (5.13 cm^3) and then, for each liquid flow rate (1.1, 2.3 and 4.2 mL/min) supplied to the micro-reactor, the corresponding contact time was calculated (4.7, 2.2 and 1.2 min). The micro-reactor was irradiated with a UV-LEDs strip (provided by *LEDlightinghut*; nominal power: 12 W/m; wavelength emission peak: 365 nm) surrounding the external surface of the cylindrical body.

The schematic diagram of laboratory scale of the continuous flow micro-reactor is shown in Fig. 1.

2.4. Ecotoxicity and data analysis

Toxicity was investigated in accordance to (Libralato et al., 2010) and (Lofrano et al., 2016) in the perspective of the best available technology (BAT) goal. The selected battery of bioassays included acute (A) and chronic (C) toxicity tests: *Lepidium sativum* (A), *Raphidocelis subcapitata* (C), and *Daphnia magna* (A) in agreement to OSPAR (2007). Toxicity included the assessment of three exposure scenarios: i) CV (10 mg/L) (pH = 5.2); CV (10 mg/L) in dark condition for 6 h at 4.7 min contact time (pH = 5.5); and iii) CV (10 mg/L) with UV treatment for 6 h at 4.7 min contact time (pH = 5.5).

2.4.1. L. sativum toxicity test

Germination index (GI, %) on L. *sativum* was determined according to (Libralato et al., 2016). The GI can assume values greater or lower than 100%, where a value equal to 100% means that the seedling average length and germination rate between a specific treatment and the negative control are the same. If values are between 80% and 120%, the effects are likely the negative controls, otherwise values >120% indicate biostimulation and lower than 80% inhibition effects.

2.4.2. R. subcapitata toxicity test

Microalgae growth inhibition test with *R. subcapitata* was carried out according to ISO (2012) (Water Quality – Freshwater Algal Growth Inhibition Test with Unicellular Green Algae. 8692 ISO, Geneva 2012). Cultures were kept in Erlenmeyer flasks. The initial inoculum contained 10^4 cells mL^{-1}. The specific growth inhibition rate was calculated considering 6 replicates exposed at 20 ± 1 °C for 72 h under continuous illumination (6000 lx). Effect data were expressed as percentage of growth inhibition.

2.4.3. D. magna toxicity test

Toxicity tests with *D. magna* were carried out according to ISO (2013) [Water Quality: Determination of the Inhibition of the Mobility of *Daphnia magna* Straus (Cladocera, Crustacea) – Acute Toxicity Test]. New-born daphnids (<24 h old) were exposed in four replicates for 24 and 48 h at 20 ± 1 °C under continuous illumination (1000 lx). Before testing, they were fed with *R. subcapitata* (300,000 cells mL^{-1}) *ad libitum*. Toxicity was expressed as the percentage of dead organism and corrected for the effects in negative controls (0 g/L ZnO) according to Abbott's formula.

2.4.4. Quality assurance/quality control and data analysis

All toxicity tests included the assessment of negative and positive controls in accordance with the specific reference method. Toxicity was expressed as percentage of effect. The significance of differences between average values of different experimental treatments and controls was assessed by the analysis of variance (ANOVA, $p < 0.05$). Statistical analyses were performed using Microsoft® Excel 2013/XLSTAT©-Pro (Version 7.2, 2003, Addinsoft, Inc., Brooklyn, NY, USA).

Toxicity data have been integrated according to Persoone et al. (Persoone and Wells, 1987) approach for natural water. The hazard classification system based on percentage of effect (PE) includes a Class I for PE < 20% (score 0, no acute toxicity), Class II for 20% ≤ PE < 50% (score 1, slight acute toxicity), Class III for 50% ≤ PE < 100% (score 2, acute toxicity), Class IV when PE = 100% in at least one test

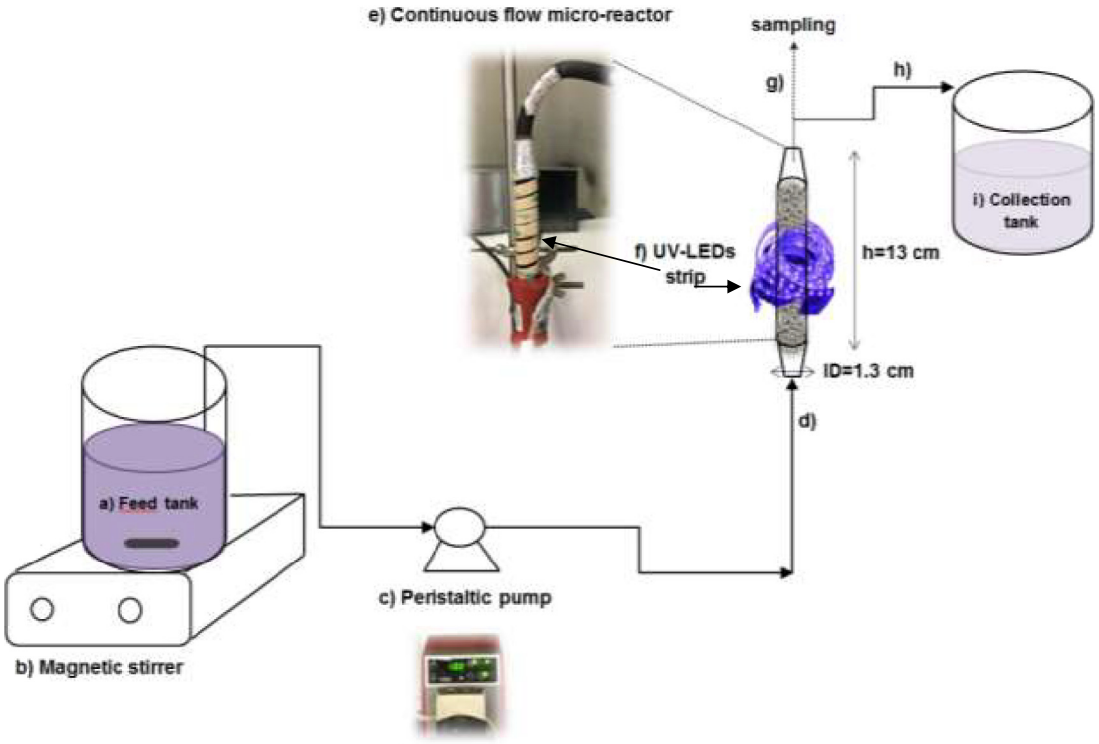

Fig. 1. Experimental set up apparatus: a) feed tank; b) magnetic stirrer; c) peristaltic pump; d) inlet of the liquid flow; e) continuous flow micro-reactor; f) UV-LEDs strip; g) sampling; h) outlet of liquid flow; i) collection tank.

(score 3, high acute toxicity) and a Class V when PE = 100% in all bioassays (score 4, very high acute toxicity). Finally, the integrated class weight score was determined by averaging the values corresponding to each microbiotest class normalised to the most sensitive organism (highest score).

3. Experimental results

3.1. Photocatalytic tests using batch reactor

Photocatalytic results in terms of CV decolourization and TOC removal as a function of irradiation time were reported in Fig. 2. As it can be noted, no CV removal is observed during the photolysis test (carried in the absence of photocatalyst and in presence of only UV light) while the presence of ZnO leads to an important decrease of CV concentration, reaching the total CV decolourization with a TOC removal equal to 96% after 120 min of UV irradiation.

In recent years, photocatalytic degradation of CV was extensively studied using several photocatalysts different from TiO_2 (Liu et al., 2018). More specifically, considering papers dealing with the use of ZnO based photocatalysts, the results obtained in the present paper in terms of photocatalytic performances are similar than those shown in the literature (Ameen et al., 2013; Tripathy et al., 2017). It is worthwhile to note that the result in terms of TOC reduction (Fig. 2) evidenced that ZnO photocatalyst was effective in the removal of reaction intermediates formed during the degradation pathway of CV.

3.2. Experimental results using the continuous flow micro-reactor

3.2.1. Adsorption tests in dark conditions using ZEO and ZnO/ZEO pellets

Adsorption experiments were performed in the continuous flow micro-reactor in order to evaluate and compare the capacity of ZEO and ZnO/ZEO in dark conditions at inlet CV concentration of 10 mg/L, flow rate of 4.2 mL/min and catalyst amount of 4 g. From the results, shown in Fig. 3, it was found that for both samples, in the first 10 min of run time, an initial fast adsorption step was observed, where around 85% of CV adsorbed was attained. In this stage the surface of both samples is still free from the crystal violet molecules and the adsorption kinetics is mainly governed by the diffusion of pollutants from the bulk solution to the sample surface (Bertolini et al., 2013; Brião et al., 2017). After, because of the adsorption sites were progressively occupied by many CV molecules, the adsorption rate decreased rapidly until the complete saturation of the adsorbent bed after 540 min of run time.

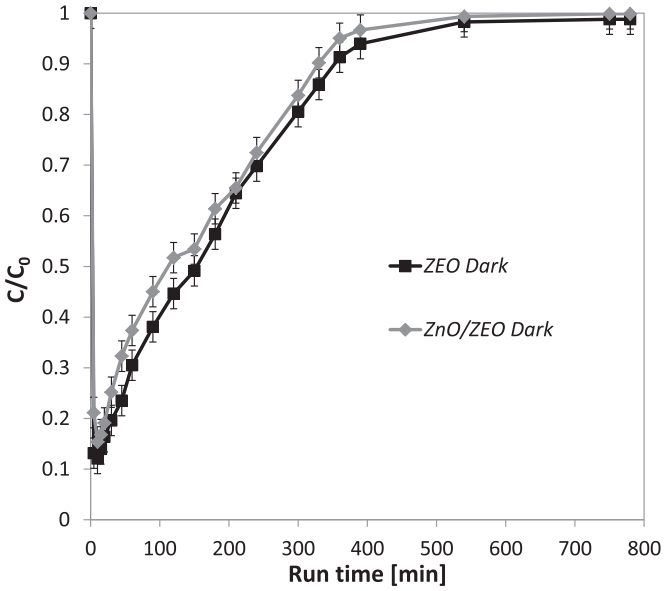

Fig. 3. Adsorption process in the continuous flow micro-reactor using ZEO and ZnO/ZEO pellets; CV inlet concentration: 10 mg/L; liquid flow rate: 4.2 mL/min; ZEO or ZnO/ZEO amount: 4 g.

Finally, the presence of ZnO into the ZEO structure did not significantly affected the adsorption performance of ZEO (Fig. 3).

3.2.2. Adsorption/photocatalytic activity tests on ZnO/ZEO pellets

Fig. 4 shows the comparison of the adsorption test in dark conditions and adsorption/photocatalytic test performed with ZnO/ZEO pellets considering an inlet CV concentration of 10 mg/L, flow rate of 4.2 mL/min and ZnO/ZEO amount of 4 g under continuous operating conditions. Comparing the curves of the dark adsorption and adsorption/photocatalysis, it is evident that, at the beginning of the process (in the first 15 min), it was reached the same CV removal value (about

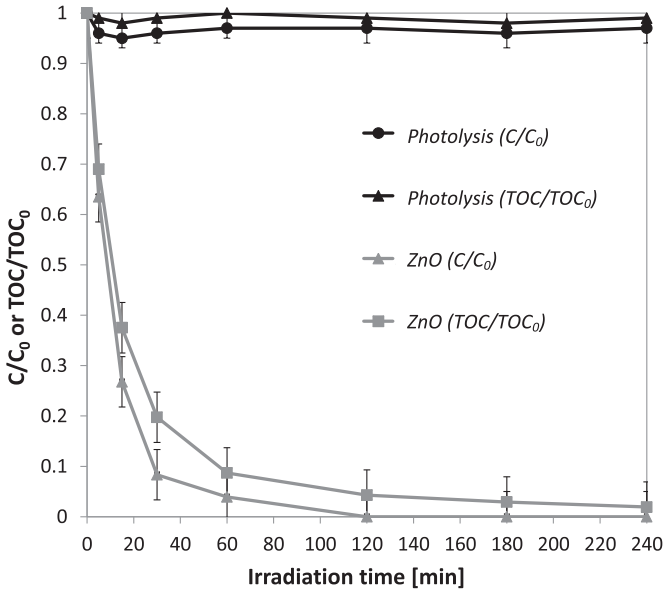

Fig. 2. Photocatalytic crystal violet degradation and mineralization under UV light using ZnO in the batch reactor; CV initial concentration: 10 mg/L; photocatalyst dosage: 3 g/L.

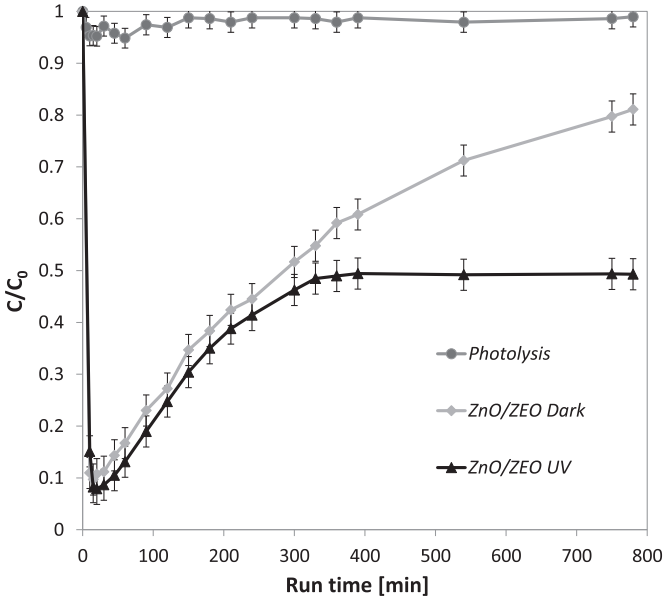

Fig. 4. Photolysis, adsorption process and adsorption/photocatalysis process in the continuous flow micro-reactor using ZnO/ZEO pellets; CV inlet concentration: 10 mg/L; liquid flow rate: 2.3 mL/min; ZnO/ZEO amount: 4 g.

90%). In dark conditions, CV concentrations tend to increase during the test time leading to the saturation of the ZnO/ZEO bed after 800 min of run time because of the continuous supply of CV molecules at the inlet of the reactor. A different behaviour was obtained in the adsorption/photocatalytic test. It is possible to observe a transient behaviour until 350 min of test and then, a steady state value of CV concentration (corresponding to a CV removal of about 51%) was achieved. This last result could be explained considering that, under UV irradiation, the generated hydroxyl radicals can oxidize the CV molecules adsorbed on the ZnO/ZEO surface, making continuously available the active sites of ZnO/ZEO for the adsorption of further CV molecules from the aqueous solution (Andriantsiferana et al., 2015). Possibly, in this way, an equilibrium condition between adsorption and photocatalytic oxidation occurred (Andriantsiferana et al., 2015).

3.2.3. Influence of the flow rate on the performances of the continuous flow micro-reactor

Adsorption/photocatalytic tests using ZnO/ZEO pellets were performed in the continuous flow micro-reactor studying the influence of the flow rate of the CV aqueous solution from 1.1 to 4.2 mL/min. The results (Fig. 5) showed that with the increase of contact time (when the flow rate decreased) there was an improvement of the performance of the system (Li et al., 2010). In the first 200 min of the test, for Q = 4.2 mL/min (contact time = 1.2 min), the adsorption kinetic is higher than that of the photocatalytic reaction. Subsequently, the equilibrium condition was achieved with a CV removal of about 20%. In the same manner, with a flow rate of 2.3 mL/min (contact time = 2.2 min), the trend of the concentration behaviour was similar to previous case obtaining a CV removal of 53% in the steady state condition. Finally, with a liquid flow rate of 1.1 mL/min (contact time = 4.7 min), the steady state value for CV removal was about 93% and it remained constant during the overall test time, evidencing that no catalyst deactivation phenomena occurred.

Finally, it was worthwhile to note that our experimental results in the continuous flow micro-reactor were obtained at contact time values sensibly lower than that typically reported in literature for continuous photocatalytic reactors (higher than 1 h) (Colombo and Ashokkumar, 2017; Vaiano et al., 2015a).

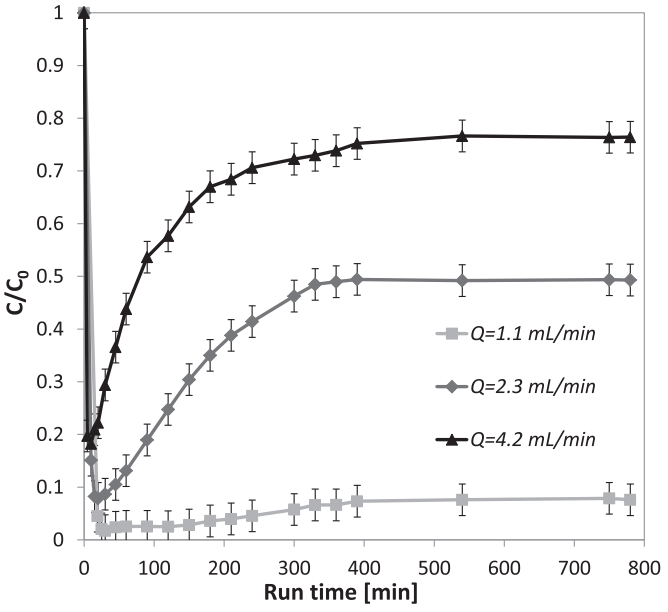

Fig. 5. Adsorption/photocatalysis process under UV light in the continuous flow micro-reactor at different liquid flow rate using ZnO/ZEO pellets; CV inlet concentration: 10 mg/L; ZnO/ZEO amount: 4 g.

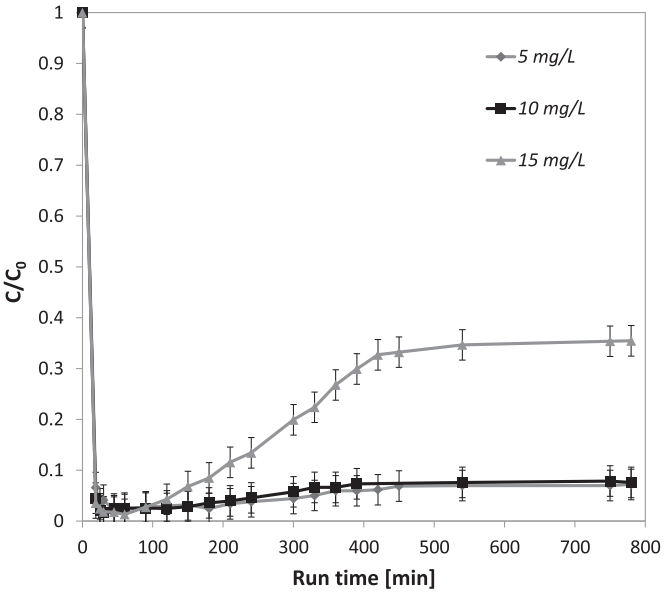

Fig. 6. Adsorption/photocatalysis process under UV light in the continuous flow micro-reactor at different inlet CV concentration using ZnO/ZEO pellets; flow rate: 1.1 mL/min; ZnO/ZEO amount: 4 g.

3.2.4. Influence of the CV initial concentration

The influence of the inlet CV concentration (in the range 5–15 mg/L) on the performance of the continuous flow micro-reactor is shown in Fig. 6. It can be observed that, up to 10 mg/L, the CV removal in the steady state conditions was similar and equal to about 93%. This last result is probably due to the availability of active catalyst surface for dye adsorption as well as for hydroxyl radical generation (Damodar and Swaminathan, 2008). At higher inlet CV concentrations (15 mg/L), up to 400 min of run time, the adsorption kinetic is probably higher than the photocatalytic one, leading to a progressive increase of residual CV concentration in solution at the outlet of the photoreactor. After 400 min of run time, the kinetic equilibrium between adsorption and photocatalysis was achieved allowing to obtain a CV removal value of about 65%, lower than that one obtained at 5 and 10 mg/L.

3.2.5. Toxicity assessment

Toxicity data were summarised in Fig. 7 for the entire battery of toxicity tests considering three exposure scenarios. Macrophytes (*L. sativum*) GI highlighted in all scenarios slight acute toxicity without no significant differences between treated and untreated CV solutions according to Libralato et al. (Libralato et al., 2016). Microalgae (*R. subcapitata*) evidenced a significant reduction of toxicity from CV solution (46% effect) to CV without UV treatment (33% effect) up to CV treated for 6 h in presence of UV (20% effect) with a whole toxicity reduction of 57%. Crustaceans were the most sensitive organisms within the battery of toxicity tests showing a 100% toxicity in the first two scenarios and a reduction of toxicity after CV treated for 6 h in presence of UV after 24 h of test duration (13% effect). These results were in line with other authors using ultrasound/heterogeneous Fenton process for CV reduction (Zhang et al., 2013) or periphyton bioreactors (Shabbir et al., 2018), but toxicity results were obtained only for the standard 24 h *D. magna* toxicity tests. We increased the contact time of *D. magna* up to 48 h evidencing an increase in the toxicity of solutions from the third scenario (73%) compared to the 24 h results suggesting that residuals and/or by-products from the administered treatments can still impair aquatic life. Particularly, in the case of *D. magna* the pH may affect toxicity, so toxicity tests were repeated adjusting the pH for all

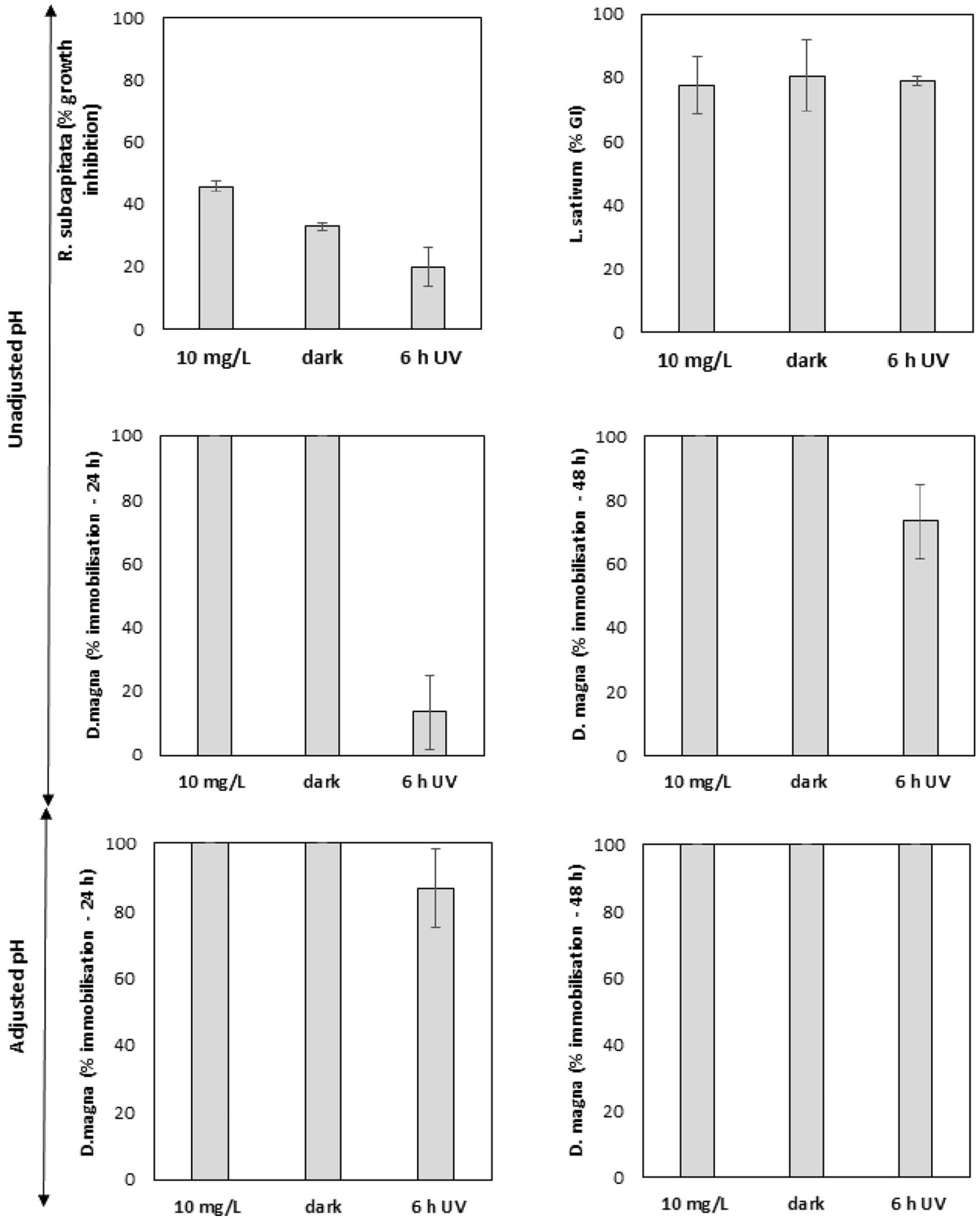

Fig. 7. Toxicity assessment of crystal violet as pure substance (10 mg/L CV), after dark adsorption (contact time: 4.7 min) and after 6 h of UV irradiation (contact time: 4.7 min) considering *R. subcapitata*, *L. sativum* and *D. magna* toxicity tests; only for *D. magna* toxicity tests were carried out with and without pH adjustment.

solutions within 7.8–8.0. According to Fig. 7 (adjusted pH), the toxicity increased up to 100% in all scenarios stating that pH can play a minor role in toxicity definition. Samples were all classified as "slight acute toxic" (Class II) suggesting that the mineralization process is still not complete because the TOC removal rate is lower than the CV degradation rate (Fig. 2). This effluent can be deemed as suitable for sewage collection discharge according to the Italian Water Act (D. Lgs 152/2006), evidencing potentialities supporting water reuse.

3.3. Mathematical modelling of the continuous flow micro-reactor under UV irradiation

3.3.1. Adsorption of CV in dark conditions on ZnO/ZEO

Adsorption experiments in dark conditions were performed in a batch system to determine the amount of CV adsorbed on ZnO/ZEO sample as a function of equilibrium dye concentration (C_e) obtained after 120 min of run time and starting from CV aqueous solutions at initial concentration in the range 2.5–35 mg/L. The solution volume and the ZnO/ZEO amount were 0.035 L and 12.5 g, respectively.

The amount of CV adsorbed onto ZnO/ZEO at equilibrium (q_e) was calculated according to the following relationship:

$$q_e = \frac{(C_0 - C_e)V}{M} \quad (1)$$

where:

C_0 is the initial dye concentration, mg/L;
C_e is the equilibrium dye concentration, mg/L;
V is the volume of solution, L;
W is the mass of ZnO/ZEO sample, g.

The obtained results are reported in Fig. 8.

The Dubinin-Radushkevich (D-R) isotherm model was applied to estimate the adsorption constants (Inyinbor et al., 2016). This isotherm is, analogue to the Langmuir type, is used to determine the occurrence of adsorption on both homogenous and heterogeneous surfaces and it is typically used for studying the adsorption of organic dyes on zeolite based materials (Bertolini et al., 2013)

D-R adsorption isotherm can be modelled by the following equation:

$$\ln q_e = \ln q_m - \beta\varepsilon^2 \quad (2)$$

where:

q_e is the amount of dye adsorbed onto ZnO/ZEO at equilibrium, mg_{CV}/g_{cat};
q_m is the D–R monolayer capacity, mg/g;
β is the activity coefficient related to mean sorption energy, mol^2/kJ^2;

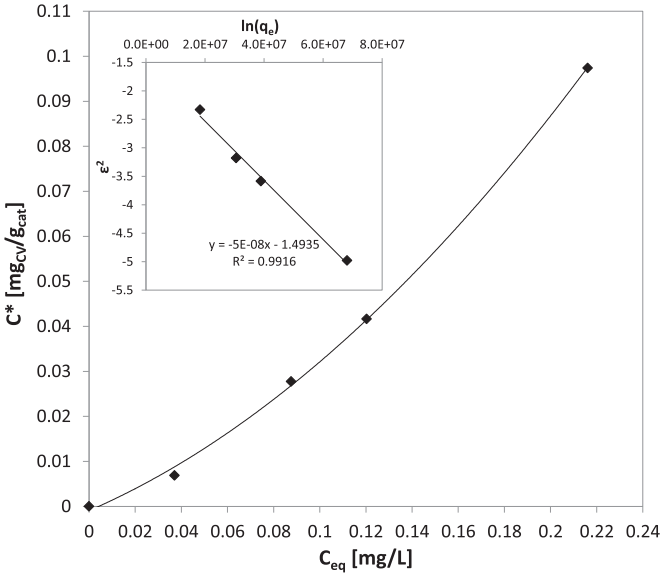

Fig. 8. Equilibrium adsorption curve of CV on ZnO/ZEO and evaluation of qm and β (insert).

ε is the Polyani potential (Polanyi, 1932), calculated using the following expression:

$$\varepsilon = RT \ln\left(1 + \frac{1}{C_e}\right) \quad (3)$$

where R is the universal gas constant (8.314 J/mol K) and T is the absolute temperature (298 K).

The plot of $\ln(q_e)$ as a function of ε^2 gives a straight line (Fig. 8 insert) where q_m and β can be derived, respectively, from the intercept and the slope of the plot line. The obtained values of q_m and β were 0.22 mg/g and $5 \cdot 10^{-8}$ mol^2/kJ^2, respectively.

3.3.2. Kinetic modelling

The kinetic model of the micro-reactor has been performed considering plug flow behaviour inside the packed bed.

Therefore, the CV mass balance under UV irradiation at steady state conditions can be written as:

$$Q\frac{dC}{dV} = r(C) \cdot \rho_{cat} \quad (4)$$

where:

Q = Total liquid flow rate, L/min;
C = CV concentration, mg/L;
V = micro-reactor volume, L;
r = CV degradation rate, mg g^{-1} min^{-1};
ρ_{cat} = bulk density of ZnO/ZEO, g/L.

The boundary condition for the Eq. (4) is:

$$V = 0 \quad C = C_0 = CV\ inlet\ concentration$$

The kinetics of CV removal could be expressed by Eq. (5):

$$-r = K \cdot f_C \quad (5)$$

where:

$$f_C = q_m \cdot e^{-\beta\left(RT \ln\left(1+\frac{1}{C}\right)\right)^2} \quad (6)$$

with:

K = kinetic constant for photocatalytic reaction, min^{-1}.

Utilizing the Eq. (5) and Eq. (6), CV mass balance can be written as:

$$Q \cdot \frac{dC}{dV} = -K \cdot q_m \cdot e^{-\beta\left(RT \cdot \ln\left(1+\frac{1}{C}\right)\right)^2} \rho_{cat} \quad (7)$$

The Eq. (7), together with the boundary condition, was solved by the Euler iterative method. Primary goal of the simulation is to estimate the constant K by fitting the experimental data reported in Fig. 9 in terms of CV removal as a function of contact time (obtained for a liquid flow rate in the range 1.1–4.2 mL/min and) with inlet CV concentration equal to 10 mg/L. The fitting procedure was done by using the least squares approach obtaining a value for K equal to $1.28 \cdot 10^{-5}$ min^{-1}. This last result evidenced that the hypothesis of neglecting the external mass transfer phenomena can be considered correct since all the experimental data as a function of contact time can be described with only one value of kinetic constant, as previously observed using a continuous fixed-bed photocatalytic reactor for the degradation of organic dyes (Vaiano et al., 2015a).

After obtaining the kinetic constant for photocatalytic reaction (K), the ability of the model to predict the experimental data was verified by comparing the CV conversion calculated from the model with experimental tests as function of different inlet CV concentrations (Fig. 10). For this purpose, a series of experiments in which the inlet CV concentration was varied from 5 to 25 mg/L were carried out. In all cases, the

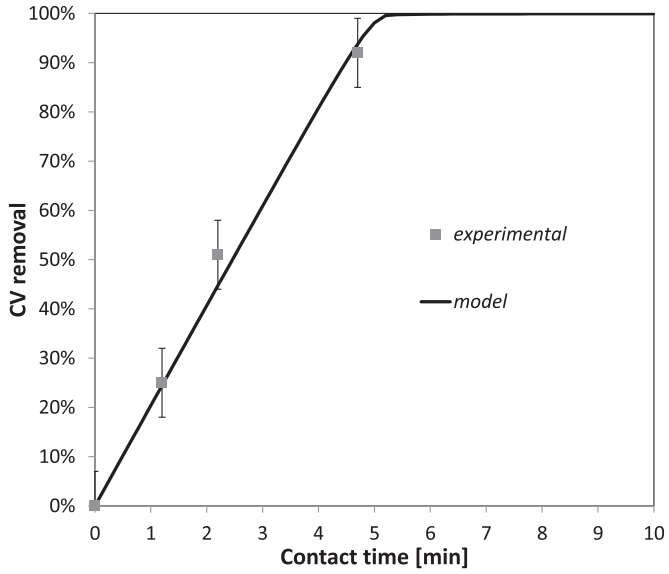

Fig. 9. CV removal as a function of contact time under UV light in the continuous flow micro-reactor; comparison between model calculation and experimental data to find the model constant K; inlet CV concentration: 10 mg/L.

calculated values are in good agreement with the obtained experimental data.

4. Conclusions

A continuous flow micro-reactor was used for the removal of CV from aqueous samples using ZnO immobilized on EO with the aim to couple adsorption and photocatalysis. The experimental results of the adsorption tests in dark conditions, demonstrated that the presence of ZnO into ZEO structure did not lead to a drastic worsening of the adsorbent ability of the material. Subsequently, experimental tests were conducted to study the performance of ZnO/ZEO pellets in the combination of adsorption/photocatalysis processes in continuous mode. The comparison between the adsorption and adsorption/photocatalytic tests showed that, the presence of UV irradiation allows to reach a steady state CV concentration value that corresponds to an equilibrium condition between adsorption and photocatalytic oxidation. Conversely to adsorption test carried out in dark conditions, the combination of adsorption/photocatalysis was able to obtain a steady state CV removal of about 51% after 350 min of run time with a liquid flow rate of 4.2 mL/min. The influence of different operating conditions such as liquid flow rate (1.1–4.2 mL/min) and inlet CV concentration (5–15 mg/L) was investigated. The results showed an improvement in performance of the system when the liquid flow rate decreased (contact time increased). With a liquid flow rate of 1.1 mL/min and an inlet CV concentration of 10 mg/L, it is possible to obtain a CV removal in stationary conditions equal to about 93% and it remained constant during the overall test time, underlining that no catalyst deactivation phenomena occurred. At higher inlet CV concentration (15 mg/L), the dye removal decreased with a steady state CV removal value of about 65%. Treated water showed a significant reduction of toxicity for microalgae (*R. subcapitata*), and no effects on macrophytes (*L. sativum*), whereas crustaceans (*D. magna*) were the most sensitive organisms to CV and its degradation products.

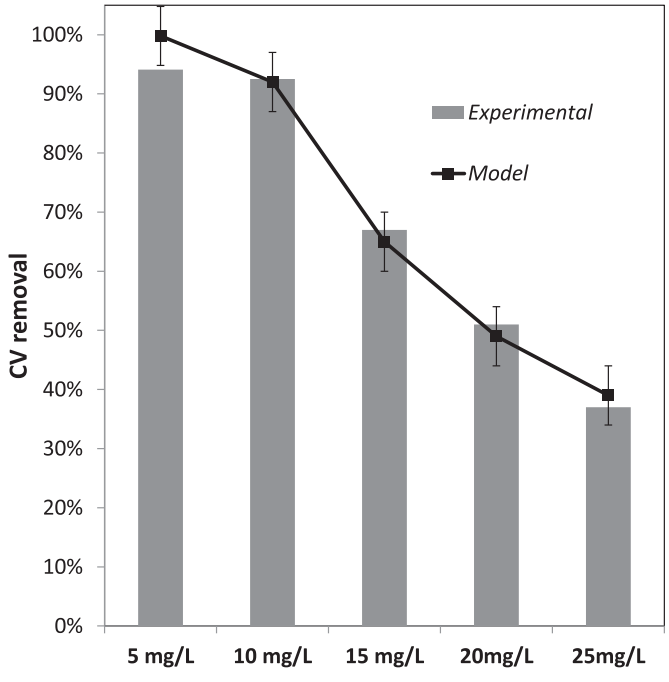

Fig. 10. Experimental and predict data under UV light in the continuous flow micro-reactor at different inlet CV concentrations; contact time: 4.7 min.

Experimental results were used to develop a preliminary kinetic model of the continuous flow micro-reactor under UV irradiation. Starting from adsorption tests carried out in a batch system, the D-R isotherm was applied in order to preliminarily calculate the adsorption parameters. Afterwards, the mathematical modelling of the photoreactor was developed by assuming that the CV molecules adsorbed on ZnO/ZEO were oxidized by photocatalysis promoted by UV light. The apparent kinetic constant for CV degradation was estimated from the experimental data obtained at different contact times. Based on these results, the accuracy of the model was tested at different CV inlet concentrations, evidencing the ability of the mathematical model to be predictive.

Acknowledgements

The authors wish to thanks “ZEOCHEM” for having provided the zeolite pellets used in the tests. Moreover, a special thank is given to Eng. Annarita Vitale for the support given in the photocatalytic tests.

References

Adak, A., Bandyopadhyay, M., Pal, A., 2005. Removal of crystal violet dye from wastewater by surfactant-modified alumina. Sep. Purif. Technol. 44, 139–144.
Ameen, S., Akhtar, M.S., Nazim, M., Shin, H.-S., 2013. Rapid photocatalytic degradation of crystal violet dye over ZnO flower nanomaterials. Mater. Lett. 96, 228–232.
Andriantsiferana, C., Farouk Mohamed, E., Delmas, H., 2015. Sequential adsorption - Photocatalytic oxidation process for wastewater treatment using a composite material TiO2/activated carbon. vol. 20.
Bertolini, T.C.R., Izidoro, J.C., Magdalena, C.P., Fungaro, D.A., 2013. Adsorption of crystal violet dye from aqueous solution onto zeolites from coal fly and bottom ashes. Orbital Electron. J. Chem. 5, 179–191 (13 pp.).
Borges, M.E., Garcia, D.M., Hernandez, T., Ruiz-Morales, J.C., Esparza, P., 2015. Supported photocatalyst for removal of emerging contaminants from wastewater in a continuous packed-bed photoreactor configuration. Catalysts 5 (77-87/1-77-87/11, 11 pp).
Brião, G.V., Jahn, S.L., Foletto, E.L., Dotto, G.L., 2017. Adsorption of Crystal Violet Dye onto a Mesoporous ZSM–5 Zeolite Synthetized using Chitin as Template. vol 508.
Cambié, D., Bottecchia, C., Straathof, N.J.W., Hessel, V., Noël, T., 2016. Applications of continuous-flow photochemistry in organic synthesis, material science, and water treatment. Chem. Rev. 116, 10276–10341.
Chanathaworn, J., Pornpunyapat, J., Chungsiriporn, J., 2014. Decolorization of dyeing wastewater in continuous photoreactors using tio2 coated glass tube media. Songklanakarin J. Sci. Technol. 36, 97–105 (9).
Chen, F., Xie, Y., Zhao, J., Lu, G., 2001. Photocatalytic degradation of dyes on a magnetically separated photocatalyst under visible and UV irradiation. Chemosphere 44, 1159–1168.
Chong, F.K., RMB, Ramli, AAB, Omar, 2017. System and Apparatus for Photodegradation of Diisopropanolamine (dipa) in Wastewater Treatment. Universiti Teknologi Petronas, Malay (pp. 15pp).
Colombo, E., Ashokkumar, M., 2017. Comparison of the photocatalytic efficiencies of continuous stirred tank reactor (CSTR) and batch systems using a dispersed micron sized photocatalyst. RSC Adv. 7, 48222–48229.
Damodar, R.A., Swaminathan, T., 2008. Performance evaluation of a continuous flow immobilized rotating tube photocatalytic reactor (IRTPR) immobilized with TiO2 catalyst for azo dye degradation. Chem. Eng. J. 144, 59–66.

Damodar, R.A., You, S.-J., Ou, S.-H., 2010. Coupling of membrane separation with photocatalytic slurry reactor for advanced dye wastewater treatment. Sep. Purif. Technol. 76, 64–71.
Dionysiou, D.D., Khodadoust, A.P., Kern, A.M., Suidan, M.T., Baudin, I., Laîné, J.-M., 2000. Continuous-mode photocatalytic degradation of chlorinated phenols and pesticides in water using a bench-scale TiO2 rotating disk reactor. Appl. Catal. B Environ. 24, 139–155.
Doong, R.-A., Hsieh, T.-C., Huang, C.-P., 2010. Photoassisted reduction of metal ions and organic dye by titanium dioxide nanoparticles in aqueous solution under anoxic conditions. Sci. Total Environ. 408, 3334–3341.
Erdei, L., Arecrachakul, N., Vigneswaran, S., 2008. A combined photocatalytic slurry reactor–immersed membrane module system for advanced wastewater treatment. Sep. Purif. Technol. 62, 382–388.
Fukahori, S., Ichiura, H., Kitaoka, T., Tanaka, H., 2003. Capturing of bisphenol A photodecomposition intermediates by composite TiO2-zeolite sheets. Appl. Catal. B Environ. 46, 453–462.
Ghaffar, A., Zhang, L., Zhu, X., Chen, B., 2018. Porous PVdF/GO nanofibrous membranes for selective separation and recycling of charged organic dyes from water. Environ. Sci. Technol. 52, 4265–4274.
Inyinbor, A.A., Adekola, F.A., Olatunji, G.A., 2016. Kinetics, isotherms and thermodynamic modeling of liquid phase adsorption of Rhodamine B dye onto Raphia hookerie fruit epicarp. Water Resour. Ind. 15, 14–27.
Janoš, P., 2003. Sorption of basic dyes onto iron humate. Environ. Sci. Technol. 37, 5792–5798.
Kamble, S.P., Deosarkar, S.P., Sawant, S.B., Moulijn, J.A., Pangarkar, V.G., 2004. Photocatalytic degradation of 2,4-dichlorophenoxyacetic acid using concentrated solar radiation: batch and continuous operation. Ind. Eng. Chem. Res. 43, 8178–8187.
Li, Y., Chen, J., Liu, J., Ma, M., Chen, W., Li, L., 2010. Activated carbon supported TiO2-photocatalysis doped with Fe ions fo continuous treatment of dye wastewater in a dynamic reactor. J. Environ. Sci. 22, 1290–1296.
Li, J., Wang, R., Su, Z., Zhang, D., Li, H., Yan, Y., 2018. Flexible 3D Fe@VO2 core-shell mesh: a highly efficient and easy-recycling catalyst for the removal of organic dyes. Sci. Total Environ. 637-638, 825–834.
Libralato, G., Volpi Ghirardini, A., Avezzù, F., 2010. Toxicity removal efficiency of decentralised sequencing batch reactor and ultra-filtration membrane bioreactors. Water Res. 44, 4437–4450.
Libralato, G., Costa Devoti, A., Zanella, M., Sabbioni, E., Micetic, I., Manodori, L., et al., 2016. Phytotoxicity of ionic, micro- and nano-sized iron in three plant species. Ecotoxicol. Environ. Saf. 123, 81–88.
Liu, P., Li, C., Han, Q., Lu, G., Dong, X., Ji, F., et al., 2014a. Phenol degradation by UV-enhanced catalytic wet peroxide oxidation process. J. Adv. Oxid. Technol. 17, 127–132 (6 pp).
Liu, S., Lim, M., Amal, R., 2014b. TiO2-coated natural zeolite: rapid humic acid adsorption and effective photocatalytic regeneration. Chem. Eng. Sci. 105, 46–52.
Liu, F.-Y., Jiang, Y.-R., Chen, C.-C., Lee, W.W., 2018. Novel synthesis of PbBiO2Cl/BiOCl nanocomposite with enhanced visible-driven-light photocatalytic activity. Catal. Today 300, 112–123.
Lofrano, G., Libralato, G., Adinolfi, R., Siciliano, A., Iannece, P., Guida, M., et al., 2016. Photocatalytic degradation of the antibiotic chloramphenicol and effluent toxicity effects. Ecotoxicol. Environ. Saf. 123, 65–71.
McCullagh, C., Robertson, P.K.J., Adams, M., Pollard, P.M., Mohammed, A., 2010. Development of a slurry continuous flow reactor for photocatalytic treatment of industrial waste water. J. Photochem. Photobiol. A Chem. 211, 42–46.
Miranda, A.C., Lepretti, M., Rizzo, L., Caputo, I., Vaiano, V., Sacco, O., et al., 2016. Surface water disinfection by chlorination and advanced oxidation processes: inactivation of an antibiotic resistant *E. coli* strain and cytotoxicity evaluation. Sci. Total Environ. 554-555, 1–6.
Nagaveni, K., Sivalingam, G., Hegde, M.S., Madras, G., 2004. Solar photocatalytic degradation of dyes: high activity of combustion synthesized nano TiO2. Appl. Catal. B Environ. 48, 83–93.
Nguyen, A.T., Juang, R.-S., 2015. Photocatalytic degradation of p-chlorophenol by hybrid H2O2 and TiO2 in aqueous suspensions under UV irradiation. J. Environ. Manag. 147, 271–277.
Ollis, D.F., Turchi, C., 1990. Heterogeneous photocatalysis for water purification: contaminant mineralization kinetics and elementary reactor analysis. Environ. Prog. 9, 229–234.
Pal, B., Kaur, R., Grover, I.S., 2016. Superior adsorption and photodegradation of eriochrome black-T dye by Fe^{3+} and Pt^{4+} impregnated TiO2 nanostructures of different shapes. J. Ind. Eng. Chem. (Amsterdam, Neth.) 33, 178–184.
Persoone, G., Wells, P., 1987. Artemia in aquatic toxicology: a review. Volucella 1.
Polanyi, M., 1932. Section III.-theories of the adsorption of gases. A general survey and some additional remarks. Introductory paper to section III. Trans. Faraday Soc. 28, 316–333.
Pozzo, R.L., Baltanás, M.A., Cassano, A.E., 1997. Supported titanium oxide as photocatalyst in water decontamination: state of the art. Catal. Today 39, 219–231.
Ray, A.K., 1999. Design, modelling and experimentation of a new large-scale photocatalytic reactor for water treatment. Chem. Eng. Sci. 54, 3113–3125.
Robinson, T., McMullan, G., Marchant, R., Nigam, P., 2001. Remediation of dyes in textile effluent: a critical review on current treatment technologies with a proposed alternative. Bioresour. Technol. 77, 247–255.
Sacco, O., Vaiano, V., Daniel, C., Navarra, W., Venditto, V., 2018a. Removal of phenol in aqueous media by N-doped TiO2 based photocatalytic aerogels. Mater. Sci. Semicond. Process. 80, 104–110.
Sacco, O., Vaiano, V., Matarangolo, M., 2018b. ZnO supported on zeolite pellets as efficient catalytic system for the removal of caffeine by adsorption and photocatalysis. Sep. Purif. Technol. 193, 303–310.
Sacco, O., Vaiano, V., Rizzo, L., Sannino, D., 2018c. Photocatalytic activity of a visible light active structured photocatalyst developed for municipal wastewater treatment. J. Clean. Prod. 175, 38–49.
Sahoo, C., Gupta, A.K., Pal, A., 2005. Photocatalytic degradation of crystal violet (C.I. basic violet 3) on silver ion doped TiO2. Dyes Pigments 66, 189–196.
Sannino, D., Vaiano, V., Ciambelli, P., Isupova, L.A., 2013. Mathematical modelling of the heterogeneous photo-Fenton oxidation of acetic acid on structured catalysts. Chem. Eng. J. 224, 53–58.
Sarno, G., Vaiano, V., Sannino, D., Ciambelli, P., 2015. Photocatalytic applications with TiO2-zeolites composites anchored on ceramic tiles. Chem. Eng. Trans. 43, 985–990.
Schuster, E.M., Wipf, P., 2014. Photochemical flow reactions. Isr. J. Chem. 54, 361–370.
Sengupta, T.K., Kabir, M.F., Ray, A.K., 2001. A Taylor vortex photocatalytic reactor for water purification. Ind. Eng. Chem. Res. 40, 5268–5281.
Shabbir, S., Faheem, M., Wu, Y., 2018. Decolorization of high concentration crystal violet by periphyton bioreactors and potential of effluent reuse for agricultural purposes. J. Clean. Prod. 170, 425–436.
Su, Y., Straathof, N.J.W., Hessel, V., Noel, T., 2014. Photochemical transformations accelerated in continuous-flow reactors: basic concepts and applications. Chem. Eur. J. 20, 10562–10589.
Susarrey-Arce, A., Hernández-Espinosa, M.A., Rojas-González, F., Reed, C., Petranovskii, V., Licea, A., 2010. Inception and trapping of ZnO nanoparticles within desilicated mordenite and ZSM-5 zeolites. Part. Part. Syst. Charact. 27, 100–111.
Tripathy, N., Ahmad, R., Song, J.E., Park, H., Khang, G., 2017. ZnO nanonails for photocatalytic degradation of crystal violet dye under UV irradiation. AIMS Mater. Sci. 4, 267–276.
Vacchi, F.I., Vendemiatti, JAdS, da Silva, B.F., Zanoni, M.V.B., Umbuzeiro, GdA, 2017. Quantifying the contribution of dyes to the mutagenicity of waters under the influence of textile activities. Sci. Total Environ. 601–602, 230–236.
Vaiano, V., Iervolino, G., 2018. Facile method to immobilize ZnO particles on glass spheres for the photocatalytic treatment of tannery wastewater. J. Colloid Interface Sci. 518, 192–199.
Vaiano, V., Sacco, O., Pisano, D., Sannino, D., Ciambelli, P., 2015a. From the design to the development of a continuous fixed bed photoreactor for photocatalytic degradation of organic pollutants in wastewater. Chem. Eng. Sci. 137, 152–160.
Vaiano, V., Sarno, G., Sannino, D., Ciambelli, P., 2015b. Photocatalytic properties of TiO2-functionalized tiles: influence of ceramic substrate. Res. Chem. Intermed. 41, 7995–8007.
Vaiano, V., Matarangolo, M., Sacco, O., Sannino, D., 2017a. Photocatalytic treatment of aqueous solutions at high dye concentration using praseodymium-doped ZnO catalysts. Appl. Catal. B Environ. 209, 621–630.
Vaiano, V., Sarno, G., Sacco, O., Sannino, D., 2017b. Degradation of terephthalic acid in a photocatalytic system able to work also at high pressure. Chem. Eng. J. 312, 10–19.
Veisi, F., Zazouli, M.A., Ebrahimzadeh, M.A., Charati, J.Y., Dezfoli, A.S., 2016. Photocatalytic degradation of furfural in aqueous solution by N-doped titanium dioxide nanoparticles. Environ. Sci. Pollut. Res. 23, 21846–21860.
Yu, K., Yang, S., Liu, C., Chen, H., Li, H., Sun, C., et al., 2012. Degradation of organic dyes via bismuth silver oxide initiated direct oxidation coupled with sodium Bismuthate based visible light photocatalysis. Environ. Sci. Technol. 46, 7318–7326.
Zhang, H., Gao, H., Cai, C., Zhang, C., Chen, L., 2013. Decolorization of crystal violet by ultrasound/heterogeneous Fenton process. Water Sci. Technol. 68, 2515–2520.
Zhang, S., Du, Y., Jiang, H., Liu, Y., Chen, R., 2017. Controlled synthesis of TiO2 nanorod arrays immobilized on ceramic membranes with enhanced photocatalytic performance. Ceram. Int. 43, 7261–7270.